PROCEEDINGS of the
23rd International Congress on Acoustics

9 to 13 September 2019 in Aachen, Germany

Analysis of low-frequency noise from wind turbines using a temporal noise code

Franck BERTAGNOLIO[(1)], Helge Aa. MADSEN[(2)], Andreas FISCHER[(3)]

[(1)]DTU Wind Energy, Denmark, frba@dtu.dk
[(2)]DTU Wind Energy, Denmark, hama@dtu.dk
[(3)]DTU Wind Energy, Denmark, asfi@dtu.dk

Abstract

This study is concerned with the modelling of low-frequency noise from wind turbines and the comparison of model predictions with experimental data. The model consists of a wind turbine aeroelastic code that can account for the effects of atmospheric turbulence combined with a noise generation model. The latter is based on the well-known Farassat 1A formulation that can compute the noise generated by aerodynamic loadings on the blades in the far-field. The results of the overall model are compared with noise measurements conducted on two wind turbines. The input parameters of the turbulence model are tuned to reflect the actual atmospheric conditions during the measurement periods. The comparisons show a relative good agreement between the predicted and measured low-frequency noise levels.

Keywords: Low-frequency noise, Wind turbine, Noise modelling, Field measurements

1 INTRODUCTION

With the deployment of increasingly larger wind turbines in rural area, but still relatively close to dwellings, wind turbine noise is one of the major environmental concerns associated to wind energy. In this respect, low-frequency noise (LFN) is pointed out as a possible threat to human health [15].

In the present study, a model is derived in order to evaluate the LFN emitted by a wind turbine. This model is based on an existing aeroelastic code that can simulate the dynamic response of a wind turbine to the incoming turbulent atmospheric wind. Here, mechanical noise is not taken into account. However, it is considered that improvements of the sound insulation of the hub contribute to make this mechanism less pronounced for modern wind turbines [14]. Two noise generation mechanisms are considered in the present model. The first one is the interaction of the blades with the atmospheric turbulence (from about 10 Hz to a few hundred Hz). The second is the blade-tower interaction with a blade passage frequency of the order of 1 Hz to a few Hz depending on the wind turbine operational mode. Both mechanisms can be explained by the unsteady aerodynamic loading on the blades which generates sound waves.

In the above-mentioned aeroelastic code, both the impact of the tower and of the atmospheric turbulence can be modelled and the subsequent loading of the blades can be calculated. Using the noise model, it is then possible to calculate the LFN generation.

The paper is organized as follows. The following section presents the several components of the proposed model that is used to simulate LFN from wind turbines. The third section is concerned with the model verification using existing LFN measurement data. Finally, conclusions are drawn.

2 A LOW-FREQUENCY NOISE MODEL FOR WIND TURBINES

The present LFN model consists of two components. The first one is the aeroelastic code HAWC2 which calculates the aeroelastic dynamic response of a wind turbine to the incoming atmospheric wind. The second is a noise generation model which converts the previously calculated aerodynamic loading on the blades into noise predictions in the far-field. Both models are detailed below. Thereafter, the inputs for the aeroelastic code in the form of the parameters defining the incoming turbulent flow field are analyzed.

2.1 The HAWC2 Aeroelastic Code

The HAWC2 code [9, 1] is a multibody aeroelastic code designed to simulate the dynamic response of a wind turbine to aerodynamic loading. It is used to predict structural vibrations and loads. Thus, it can be used as a design tool for wind turbines. Each individual blade is discretized along its span into a number of elementary beams. On each of these elements, the Blade Element Momentum theory by Glauert [7] is applied in order to calculate the aerodynamic loading resulting from the incoming wind and the rotation of the blades. A variety of unsteady atmospheric loadings (e.g. turbulence, gust) and other flow characteristics (e.g. wake from an upwind turbine, tower flow disturbances and wake) can be accounted for in this model.

In particular, the model used to simulate atmospheric turbulence is the Mann model [12, 13]. It is based on a spectral description of the turbulent flow field which is converted into a random turbulent velocity flow field. The latter is convected together with the main wind speed assuming frozen turbulence (see Section 2.3 for more details).

The flow disturbances created by the tower are altering the aerodynamic loading on the blades. The modified flow upwind of the tower can be calculated and is used to simulate the case of an upwind rotor. The downwind tower wake flow deficit can also be simulated, together with its impact on the blades of a downwind rotor (see details in Section 2.3).

The HAWC2 code calculates in the time domain the aerodynamic loading on each of the discrete blade elements in term of aerodynamic lift and drag. The resulting time-series for these quantities can be used to compute the noise emissions as described in the next section.

2.2 Formulation 1A Model by Farassat

The method developed by Farassat [5] is shortly speaking a more advanced expression of Ffowcs Williams-Hawking solution [6] of the original Lighthill's acoustic analogy [10]. Its main asset lies in the fact that it yields relatively accurate numerical evaluation of the acoustic pressure generated by a surface or object moving in a fluid and interacting with it through some fluctuating aerodynamic loading, as well as the acoustic pressure resulting from the displacement of the fluid created by the thickness of the object itself. Nevertheless, the latter mechanism is negligible in the context of wind turbine operation. This noise generation model has been implemented into the HAWC2 code as described in a previous publication [4].

Note that this model predicts time-series of acoustic pressure at prescribed locations away from the noise sources (in our case, the discrete beam elements along the blade, see above) in the far-field. This time-series can be Fourier transformed to obtain noise spectra, much in the same way that acoustic pressure recordings from a microphone in the field are converted to sound pressure level spectra.

It should be noted here that noise propagation is not included in the present model. Only the geometrical spreading of the noise as it radiates away from the turbines is accounted for. Nevertheless, the noise data that are analyzed later in this paper are measured relatively close to the test turbines that are investigated. Therefore, it is believed that other noise propagation mechanisms (e.g. air absorption) are relatively negligible.

2.3 Wind Velocity and Atmospheric Turbulence

As described earlier, the LFN generation is driven by two main mechanisms which are discussed in this section.

Firstly, the blade-tower interaction can occur in two distinct configurations. In the case of an upwind rotor, the flow disturbances by the tower are simulated using a model based on the potential flow solution of the flow around a circular cylinder as described in [9]. In the case of a downwind rotor, the tower shadow model (the so-called JET wake model) is based on the boundary layer solution for a jet flowing into a fluid at rest and is described in detail in the paper by Madsen *et al* [11].

Secondly, the Mann model [12, 13] is used to simulate the atmospheric turbulence. This model requires three input parameters:

- the turbulent energy content in the form of $\alpha\varepsilon^{2/3}$ where ε is the turbulent kinetic energy dissipation rate and α a scaling constant,
- the turbulence integral length scale L, and
- the anisotropy factor Γ.

The definition of the numerical values assigned to each of these parameters for the simulations is discussed below.

It is found that the anisotropy factor Γ has little influence on the results. The value $\Gamma{=}3.9$ from the IEC 61400-1 standard for wind turbine design requirements is used [2].

A recent publication by Kelly [8] shows that the integral length scale L can be evaluated with reasonable accuracy from standard 10 mins average anemometer measurements using the following approximation:

$$L \approx \sigma_u/(dU/dz) \tag{1}$$

where σ_u is the shear stress of the main wind velocity component and the denominator is the wind shear. For the experimental data considered in this article, both values will be extracted from mast sonic anemometers. An anemometer located at hub height is used for the shear stress. The wind shear is also evaluated at hub height using the 6 other anemometers along the mast height (see below).

In the same above paper [8], the ratio between the measured σ_u^2 and the theoretical variance of the velocity components σ_{iso}^2 for isotropic turbulence is found to be approximately equal to 5/3. This approximation should remain valid as long as the surrounding terrain is not too complex (as it is the case for the terrain around the Risø test station where the two turbines considered in the next section are located). Integrating the velocity spectrum derived from the well-known von Kármán energy spectrum yields the following value for the variance of an isotropic turbulent flow:

$$\sigma_{\text{iso}}^2 = 0.688\,\alpha\varepsilon^{2/3}L^{2/3}$$

Combining the previous equation with the above mentioned ratio and length scale approximation gives the following approximation for the remaining Mann model's input parameter:

$$\alpha\varepsilon^{2/3} = 0.872\,\sigma_u^2 L^{-2/3} \approx 0.872\,\sigma_u^{4/3}(dU/dz)^{2/3} \tag{2}$$

Concerning, the inflow wind velocity impinging the turbine rotor, a logarithmic profile is enforced in the calculations presented later in this article. Denoting U_H the velocity at hub height $z{=}H$, where z is the elevation from the ground, then the wind velocity reads:

$$U(z) = U_H \ln(z/z_0)/\ln(H/z_0) \tag{3}$$

where z_0 is the roughness length which is tuned to fit the 10 mins averaged wind velocity profiles measured by the met mast anemometers. From these values, the wind shear at hub height can be evaluated as:

$$dU/dz(z{=}H) = U_H/\big(H\ln(H/z_0)\big) \tag{4}$$

which in turn is used to compute the turbulence length scale L according to Eq. (1) and $\alpha\varepsilon^{2/3}$ according to Eq. (2) as inputs of Mann model.

The procedure to quantitatively define the above parameters to be used for modelling specific noise measurement data in the next section is described below. Wind velocity profiles are evaluated from anemometers along the met mast height using 10 mins average time-series. The roughness length is tuned so that the average measured wind speed values match the computed value using Eq. (3). Thereafter, the wind shear can be computed using Eq. (4). Its value is evaluated at hub height. It is important to note here that the influence of the wind shear on L and $\alpha\varepsilon^{2/3}$ as defined by Eqs. (1) and (2) is considered as a characteristics of the particular atmospheric conditions for the day (or rather the few hours) of the considered measurement campaign. It is thereby assumed that the atmospheric boundary layer conditions remain qualitatively constant during that period of time. The wind velocity at hub height is averaged over the whole measurement campaign and the resulting hub height wind shear computed with Eq. (4) is considered as representative of the specific atmospheric conditions for that day, and this latter quantity is used in Eqs. (1) and (2). In parallel, the met mast anemometer at hub height is used to compute $\sigma_u(H,U_H)$ and a linear regression is performed based on 10 mins averaged of the wind speed at hub height. The value of σ_u used in Eqs. (1) and (2) to evaluate L and $\alpha\varepsilon^{2/3}$ makes use of this linear regression using the wind speed of interest for each specific noise measurement data set (which are binned according to the mean wind speed at hub height, see next section).

3 MODEL VERIFICATION

The results of the proposed model are confronted to experimental data that were acquired when measuring noise from two wind turbines.

3.1 Risø Test Station for Wind Turbines

Noise measurements were conducted at the DTU-Risø campus on two wind turbines. The first one is the NordTank NTK 500 with a 41 m rotor diameter and a hub height of 36 m. It is stall-regulated and operates with a constant rotational speed. The second is a Vestas V52 pitch-regulated turbine with a rotor diameter of 52 m and a hub height of 44 m.

Both turbines are equipped with various sensors that record the operational conditions such as rotational speed, blade pitch, etc. In addition, met masts are located near the turbines. Wind speeds and directions, temperature and other atmospheric quantities are measured at various heights up to the tip of the wind turbines. The sampling frequencies for the acquisition systems are 35 Hz for the NTK 500 and 50 Hz for the V52 turbine.

Concerning the noise measurements, 8 ground microphones are placed on plywood boards around the turbines. The microphones and the acquisition system are described in details in a previous article [3] where some of the results of the experimental campaigns for the NTK 500 turbine were investigated. The set-up is identical for the V52 measurement campaign.

3.2 Wind Velocity Profiles and Turbulence Parameters

As explained earlier, the results of the LFN model primarily depend on the inputs to the Mann model which reduce to two main parameters: wind shear and turbulence intensity at hub height. Wind shear is computed from the mean wind speed profile during the considered campaign, assuming that it does not significantly change during that period. Figs. 1(a-c) displays the average wind velocity profiles, as measured by the met masts anemometers, using a binning from the nacelle anemometers for the NTK turbine on Oct. 15-16 and 23 for the two first figures, respectively, and for the V52 turbine for the third one. From this measured data, logarithmic velocity profile can be fitted by tuning the roughness length z_0 in Eq. (3) for each individual case.

The second parameter of interest, the standard deviation σ_u, is evaluated from 10 mins time-series from met mast anemometers at hub height and a linear regression is used in order to evaluate its actual value as a function of wind speed. Both the 10 mins variances and the linear regression are plotted in Fig. 2(a-b) for the four cases considered above.

Using the above measurement data, the parameters used as input for the Mann's turbulence model are computed according to the procedure described in Section 2.3 and quantitative values are summarized in Table 1 for the different measurement campaigns.

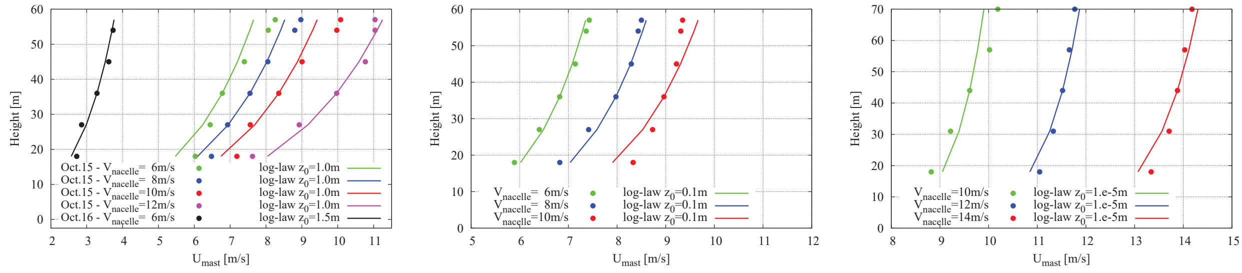

(a) NTK turbine on Oct. 15 & 16 - z_0 = 1.0 & 1.5 m

(b) NTK turbine on Oct. 23 - $z_0 = 0.1$ m

(c) V52 turbine - $z_0 = 10^{-5}$ m

Figure 1. Wind velocity profiles (Lines: logarithmic profiles according to Eq. (3), Points: averaged velocities measured by met mast anemometers and binned using nacelle anemometer).

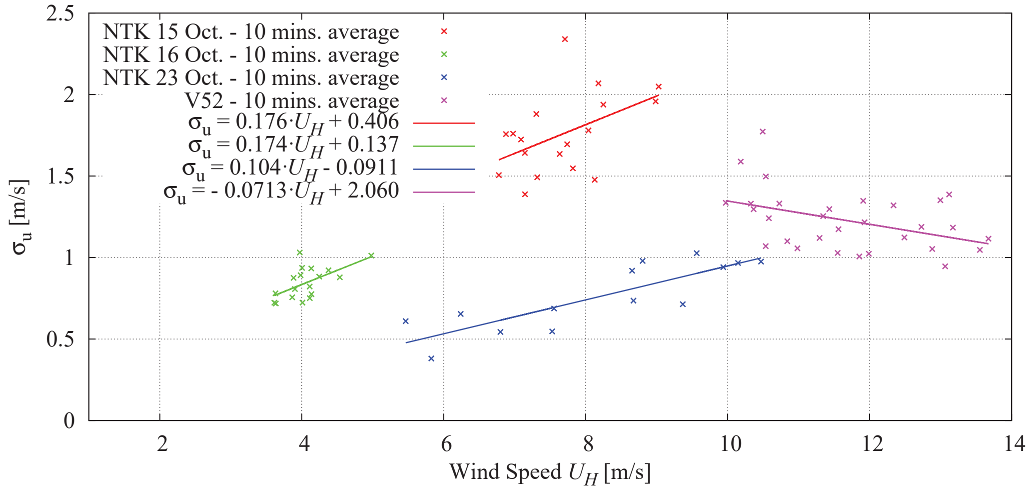

Figure 2. σ_u as a function wind speed as measured by met mast anemometer at hub height for NTK 500 and V52 measurement campaigns.

3.3 Low-Frequency Noise Spectra

Noise measurements, as well as background noise, for the NTK and the V52 turbines are reported in Figs. 3(a-c) and 3(d), respectively. It can be observed that background noise contaminates the NTK turbine noise measurements in the 40-100 Hz frequency band, mostly at low wind speeds, as far as the broadband noise spectra are concerned. This part of the background noise probably originates from nearby road traffic, and possibly vegetation noise. In addition, numerous spurious peaks are also observed and these may be attributed to machinery noise from the nacelle. Noise measurements for the V52 turbine also exhibit such peaks in this frequency range. The peaks present in the background noise probably also originate from the wind turbine nacelle where internal machinery still operates during standstill (e.g. cooling fans).

Background noise also contaminates the measurements below 20 Hz except for the NTK case on Oct. 16. It is attributed to vegetation or ambient noise which is less predominant on Oct. 16 because of the relative lower wind speeds that day (see Fig. 2). Note however that the microphones' manufacturer provides a calibration sheet down to 20 Hz with a very flat response function down to that frequency. Nevertheless, the measurement data appear consistent with the model below this frequency, unless there is a surmised high background noise

Table 1. Turbulence parameters for experimental campaigns at considered wind speeds.

Campaign/Wind speed	z_0 [m]	$dU/dz(H)$ [s^{-1}]	σ_u [m/s]	L [m]	$\alpha\varepsilon^{2/3}$ [m$^{4/3}$/s^2]
NTK Oct. 15 - $U_H = 6$ m/s	1.0	0.0595	1.511	25.41	0.2305
NTK Oct. 15 - $U_H = 10$ m/s			2.109	35.46	0.3595
NTK Oct. 16 - $U_H = 4$ m/s	1.5	0.0355	1.115	31.41	0.1090
NTK Oct. 23 - $U_H = 6$ m/s	0.1	0.0388	0.565	14.57	0.0466
NTK Oct. 23 - $U_H = 10$ m/s			0.889	22.93	0.0854
V52 - $U_H = 10$ m/s	10^{-5}	0.0174	1.347	77.47	0.0870
V52 - $U_H = 14$ m/s			1.061	61.06	0.0633

which is also consistent with the measured wind turbine noise spectra (see above).

The model results, using the input parameters for each test case as defined earlier, are also displayed in the figures. It can be seen that there exists a general good qualitative agreement between measurements and model results (leaving out background noise contaminations). The model reproduces correctly the quantitative increase of LFN as a function of wind speed, although in some cases and some frequency ranges discrepancies between the actual noise levels are observed.

4 CONCLUSIONS

A model for calculating the LFN emitted by wind turbines is proposed. One of the components of this model is the Mann turbulence model used to simulate atmospheric turbulence. This latter model input parameters are tuned using experimental data extracted from met mast measurements near the turbines that are investigated. The Mann model is the primary component of the proposed model, in the sense that it is used to define the turbulent flow field that impact the turbines and generate noise by interacting with the blades. The other components of the model, which consist of the wind turbine aeroelastic model together with the generation of LFN from aerodynamic fluctuations on the blades, are also described in this paper.

The results of the combined model are compared to existing noise measurements on two wind turbines. There is a fair agreement between the model predictions and the experimental data. However, this is a preliminary study and additional turbines must be investigated to validate the model. Indeed, the two turbines considered in the present study are relatively old and small compared to modern MW-size turbines. Furthermore, the contribution of the blade-tower interaction to the LFN emissions, even if these are included in the present calculations, remains to be investigated in more detail. More specifically, the LFN emission from downwind rotors is of particular interest.

ACKNOWLEDGEMENTS

This study was conducted as part of the program "Cross-Cutting Activities" internally funded by DTU Wind Energy.

The authors would like to thank Kasper Clemmensen, Karen Enevoldsen, Per Hansen, Uwe S. Paulsen, Claus B. M. Pedersen and Michael Rasmussen from DTU Wind Energy for participating in the design of the experiment, preparing the hardware and acquisition software, and conducting the field measurements.

REFERENCES

[1] HAWC2 Aeroelastic Simulation of Wind Turbines. http://www.hawc2.dk. Accessed: 2017-04-28.

[2] International Standard, Wind Turbines - Part 1: Design Requirements. IEC 61400-1, International Elec-

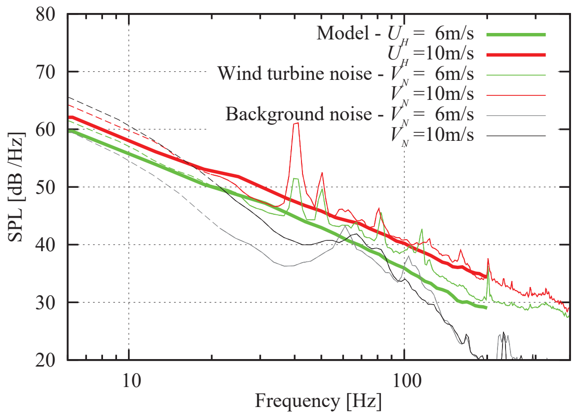

(a) NTK turbine 15 Oct. - $z_0 = 1.0$ m

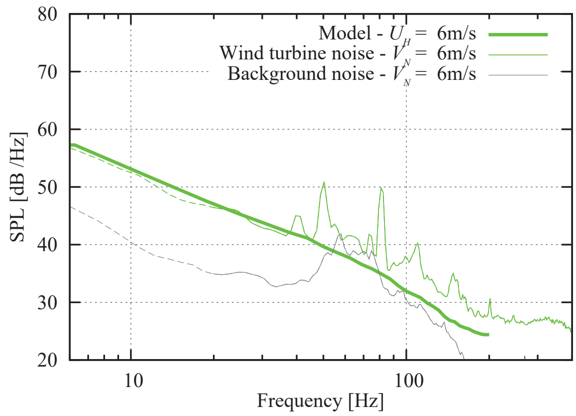

(b) NTK turbine 16 Oct. - $z_0 = 1.5$ m

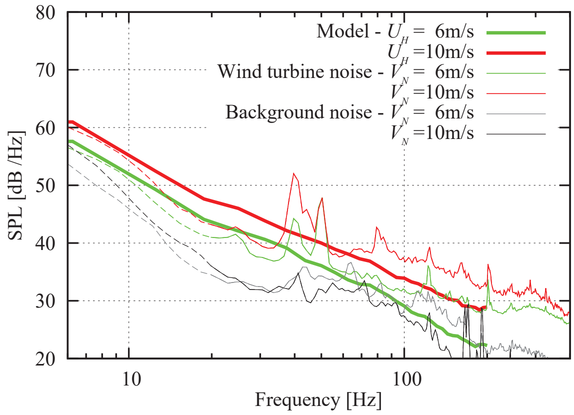

(c) NTK turbine 23 Oct. - $z_0 = 0.1$ m

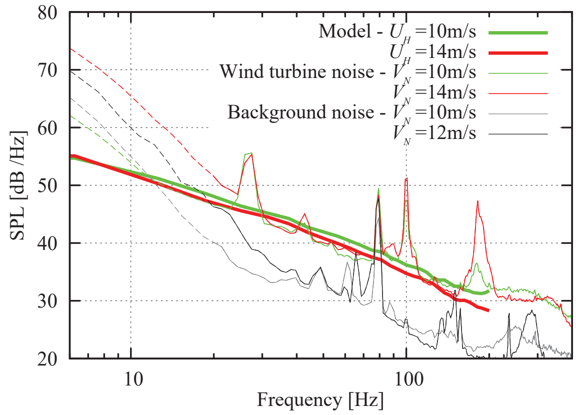

(d) V52 turbine - $z_0 = 10^{-5}$ m

Figure 3. Sound pressure level spectra for the NTK and V52 turbines (Thick lines: model, Thin lines: measurements, Dashed lines: frequencies below 20 Hz for measured spectra).

trotechnical Commission, Geneva (CH), Aug. 2005.

[3] F. Bertagnolio, H. A. Madsen, and A. Fischer. A Combined Aeroelastic-Aeroacoustic Model for Wind Turbine Noise: Verification and Analysis of Field Measurements. *Wind Energy*, 20(8):1331–1348, 2017.

[4] F. Bertagnolio, H. A. Madsen, and A. Fischer. A Temporal Wind Turbine Model for Low-Frequency Noise. In *InterNoise17*, INTER-NOISE and NOISE-CON Congress and Conference Proceedings, pages 5025–5033, Hong Kong, China, August 2017. INCE (publisher).

[5] F. Farassat and G. P. Succi. A Review of Propeller Discrete Frequency Noise Prediction Technology with Emphasis on Two Current Methods for Time Domain Calculations. *J. Sound Vib.*, 71(3):399–419, 1980.

[6] J. E. Ffowcs Williams and D. L. Hawkings. Sound Generated by Turbulence and Surfaces in Arbitrary Motion. *Philosophical Transactions of the Royal Society*, A264(1151):321–342, 1969.

[7] H. Glauert. *Airplane Propellers*, volume In: Aerodynamic Theory Volume IV. Springer, Berlin, Heidelberg, 1935.

[8] M. Kelly. From Standard Wind Measurements to Spectral Characterization: Turbulence Length Scale and Distribution. *Wind Energy Science*, 2018. (Available online: https://www.wind-energ-sci-discuss.net/wes-2018-14/).

[9] T. J. Larsen and A. M. Hansen. How 2 HAWC2, The User's Manual. Tech. Rep. RISØ-R-1597(ver.3-1), Risø-DTU, Roskilde, Denmark, December 2007.

[10] M. J. Lighthill. On Sound Generated Aerodynamically. I. General Theory. *Proceedings of the Royal Society London A*, 211(1107):564–587, 1952.

[11] H. A. Madsen, J. Johansen, N. N. Sørensen, G. C. Larsen, and M. H. Hansen. Simulation of Low Frequency Noise from a Downwind Wind Turbine Rotor. In *45th AIAA Aerospace Sciences Meeting and Exhibit*, AIAA 2007-623, Reno (NV), January 2007.

[12] J. Mann. The Spatial Structure of Neutral Atmospheric Surface-layer Turbulence. *Journal of Fluid Mechanics*, 273:141–168, 1994.

[13] J. Mann. Wind Field Simulation. *Probabilistic Engineering Mechanics*, 13(4):269–282, 1998.

[14] S. Oerlemans, P. Sijtsma, and B. M. López. Location and Quantification of Noise on a Wind Turbine. *J. Sound Vib.*, 299(5-6):869–883, 2007.

[15] E. Pedersen and K. P. Waye. Perception and Annoyance Due to Wind Turbine Noise - A Dose–Response Relationship. *Journal of the Acoustical Society of America*, 116(6):3460–1418, 2004.